Tellus (1994), 46A, 229–241
Printed in Belgium – all rights reserved

TELLUS
ISSN 0280–6495

Absorption feedback in stratocumulus clouds Influence on cloud top albedo

By REINOUT BOERS* and ROSS M. MITCHELL, *CSIRO Division of Atmospheric Research, Private bag No. 1, Mordialloc, Victoria 3195, Australia*

(Manuscript received 10 September 1992; in final form 27 September 1993)

ABSTRACT

This paper proposes a feedback mechanism which modifies the enhancement of cloud top albedo expected from an increased concentration of cloud condensation nuclei (CCN). The mechanism is based on the thermodynamic tendency of the cloud to stabilize itself against changes in the absorption of solar radiation. For optically thin clouds, this absorption feedback leads to a reduction in the anticipated albedo enhancement, while for optically thick clouds, an amplification of the albedo enhancement is predicted. The likely impact of this effect on the radiative forcing of climate due to changes in CCN and hence cloud top albedo is discussed.

1. Introduction

Marine boundary layer clouds have been the focus of much attention over recent years, due in part to their possible role in moderating the earth's climate. In particular, extensive quasi-permanent decks of stratocumulus clouds are prevalent in a number of areas around the globe (e.g., Randall, 1984). These clouds are highly efficient reflectors of incoming shortwave solar energy, but emit in the longwave at a temperature not very different from the surface. Hence their net effect is to cool the earth-atmosphere system.

An important aspect of the role of these clouds in relation to climate is the dependence of cloud top albedo on the notional droplet size. Since the latter is influenced by the local concentration of cloud condensation nuclei (CCN), changes in CCN have the potential to affect the cloud top albedo, and hence to modulate the input of radiant energy to the planet. Twomey (1977) and Twomey et al. (1984) investigated this effect in the context of the impact of increasing pollution on cloud optical depth. They found that increasing pollution leads to an increase in droplet concentration with an associated decrease in droplet size. These changes act to increase the cloud optical depth, which in most circumstances causes an increase in cloud top albedo. This chain of events has since become known as the "Twomey effect" (Hudson, 1991).

Experimental confirmation of the effect is seen in the ship track measurements of Radke et al. (1989). Using a combination of satellite and in situ observations, they found unambiguous increases in droplet concentration and cloud top albedo along the tracks. These effects were explained in terms of enhanced CCN number densities due to emission from ships.

The effect of CCN on cloud top albedo was linked into the climate change debate by Charlson et al. (1987), who proposed that CCN originating from oceanic phytoplankton could act as a significant modulator of cloud albedo. This opened the possibility of a regulatory feedback loop, since the primary production rate is governed by ocean temperature. Furthermore, Charlson et al. (1992) highlighted the quantitative significance of this effect by suggesting that a 30% increase in global CCN concentration may give rise to a forcing of $-2\ \mathrm{W\ m^{-2}}$, one half of the "greenhouse" forcing of $+4\ \mathrm{W\ m^{-2}}$ due to doubled CO_2.

Overlooked in the previous work is the possibility

* Corresponding author.

of internal change to the cloud as a result of the externally imposed change in microphysics. For example, in the studies of Twomey and co-workers cited above, it was assumed that the cloud optical depth may be fixed simply by specifying the initial droplet concentration, liquid water content, and cloud height. In reality, modification of the cloud microphysics implied through changes in droplet size and concentration will affect the absorption of solar energy within the cloud, thus changing the internal thermodynamic balance. This change in thermodynamic state then alters the microphysics, establishing a feedback loop which further modifies the radiative transfer characteristics. Two possibilities exist: the feedback is negative, and responds by partly or wholly negating the initial perturbation; or the feedback is positive, and responds by enhancing the initial perturbation.

This paper takes a first step in exploring the nature and significance of the internal feedback mechanism outlined above. This is pursued using a combination of thermodynamic and radiative transfer models. In brief, microphysical arguments are used to relate quantities of radiative significance such as optical depth and droplet radius, to thermodynamic parameters. Attention is focused on the "mixing parameter", which quantifies the extent to which dry air is entrained into the cloud. This parameter provides the necessary link between the convective and radiative structure of the cloud. Next, radiative transfer models are employed to investigate whether perturbations in droplet concentration enhance or diminish solar absorption in the cloud. It is found that the absorption in optically thin clouds is enhanced, while that in optically thick clouds is diminished. Remarkably, in each case the feedback acts to stabilize the solar absorption. The consequences for cloud albedo once again depend on cloud optical depth. For optically thin clouds, the feedback decreases the albedo, while for optically thick clouds, the albedo is further enhanced. The paper concludes with a discussion of the impact of these findings on climate.

2. Impact of mixing on cloud microphysics

The evaluation of the significance of the proposed internal feedback mechanism depends on being able to relate the thermodynamic effects of modified solar absorption to some consequent change in cloud microphysics. The thermodynamic effect considered here is the change in the degree of convective mixing in the cloud. Hence the goal of this section is to derive functional relationships expressing the link between changes in mixing and changes in microphysics. This then allows the derivation of the functional dependence of parameters which influence the radiative transfer in the cloud.

2.1. Mixing

Mixing in cloudy boundary layers has been discussed by Betts (1985, and references therein). Betts introduced a mixing parameter β, defined so as to track the height variation of conserved variables such as equivalent potential temperature, liquid water potential temperature and total water mixing ratio, as a result of mixing between the cloudy boundary layer and the overlying dry atmosphere. In particular,

$$\beta = \frac{\mathrm{d}p_*}{\mathrm{d}p}, \tag{1}$$

where p is the pressure at a given level, and p_* is the saturation pressure of air at that level. Hence, $p_* < p$ in a given air parcel implies subsaturation, whilst $p_* > p$ indicates saturation and cloud formation.

It is important to distinguish between mixing within the cloudy boundary layer itself, and mixing as a process involving the boundary layer and the overlying dry stable air. This last process is often referred to as entrainment. With each mixing process is associated a time scale: t_b for internal boundary layer mixing; t_e for entrainment. These time scales express the relative strength of each process, and hence determine the value of the mixing parameter. For example, when $t_b \ll t_e$, boundary layer mixing is dominant. Entrained parcels will be rapidly and uniformly mixed throughout the boundary layer, so that the lifting condensation level will be independent of height, and hence $\beta = 0$. When the mixing time scales are comparable, uniform mixing of entrained parcels is no longer possible. A substantial number of entraining warm parcels will be found near the top of the boundary layer, so that the saturation level in the boundary layer will increase with altitude, so that $\beta > 0$. In the special case $\beta = 1$, there is a constant

offset between the pressure at any level within the boundary layer, and the associated saturation level pressure. For an air parcel which is initially just subsaturated, this implies that there is exactly sufficient mixing of entrained air to maintain the initial degree of subsaturation as the parcel is raised vertically, and thus cloud formation is inhibited. Hence, for a cloud to form in the rising air column, the condition $0 \leqslant \beta \leqslant 1$ is necessary. Values of β for boundary layer clouds range from 0.3 to 0.4 (Boers and Betts, 1988; Betts and Boers, 1990; Boers et al., 1991). Somewhat smaller values are inferred from earlier observations of the liquid water content of stratus clouds (Nicholls, 1984; Nicholls and Leighton, 1986).

Of particular relevance to this work is the variation of liquid water mixing ratio with height,

$$w(z) = (1-\beta)\, w_A(z). \tag{2}$$

Assuming linear vertical variation of w_A, the adiabatic liquid water mixing ratio, then

$$w(z) = (1-\beta)\, A_d(z - z_B), \tag{3}$$

where A_d is the vertical gradient of the adiabatic liquid water mixing ratio and z_B is the height of cloud base. Clearly, when β is small the liquid water mixing ratio remains close to its adiabatic value. On the other hand when β approaches 1, the liquid water falls to zero, as expected from the preceeding discussion.

2.2. *Microphysics*

The relation between liquid water content and mixing parameter given in eq. (3) provides the essential link between thermodynamics and microphysics. However, in order to use it to determine parameters of radiative consequence, it is necessary to specify the size distribution of the water droplets. If we assume that the size spectrum follows a gamma distribution (e.g., Diermendjian, 1969), and that the droplet number density is N, then the Appendix shows that the cloud optical depth τ and effective droplet radius r_{eff} may be written

$$\tau = C_1(1-\beta)^{2/3}\, N^{1/3} h^{5/3}, \tag{4}$$

$$r_{eff}(z) = C_2(1-\beta)^{1/3}\, (z - z_B)^{1/3}\, N^{-1/3}, \tag{5}$$

where h is the geometrical cloud thickness $z_T - z_B$, with z_T the cloud top height. Although a gamma distribution was assumed in the derivation given in the *Appendix*, the functional forms of (4) and (5) do not depend on the size distribution. For example, it is easy to show that identical functional dependences result for a monodispersion, although the constants C_1 and C_2 are modified.

Eq. (4) shows that τ is proportional to $N^{1/3}$, $(1-\beta)^{2/3}$, and $h^{5/3}$. The first factor is well-known. The second indicates that mixing reduces the value of optical depth, while the third suggests a dependence on h which is much larger than the $\tau \propto h$ found by Twomey (1977).

The effective radius r_{eff} decreases with increased mixing, and with increased droplet number density. Figs. 1 and 2 show vertical profiles of r_{eff}. Fig. 1 shows the sensitivity with respect to changes in N, while Fig. 2 displays its variability with respect to β. These figures indicate large changes in the effective radius in response to changes in either droplet number density or mixing parameter.

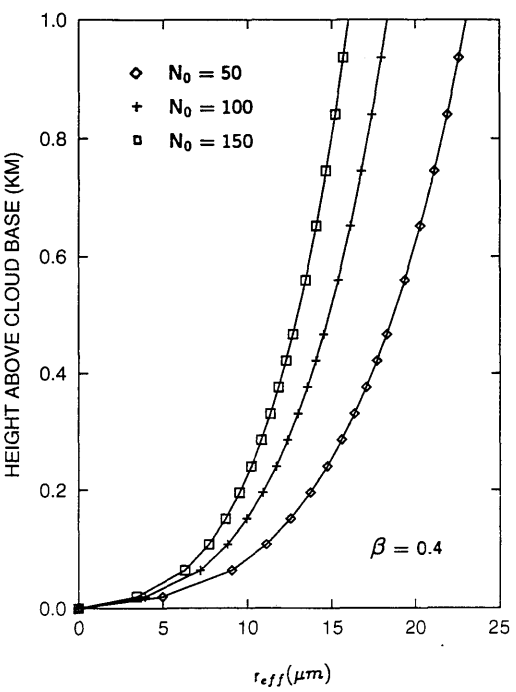

Fig. 1. Variation of the effective radius of droplets as a function of height above cloud base for different values of droplet concentration N. The mixing parameter β was set to 0.4.

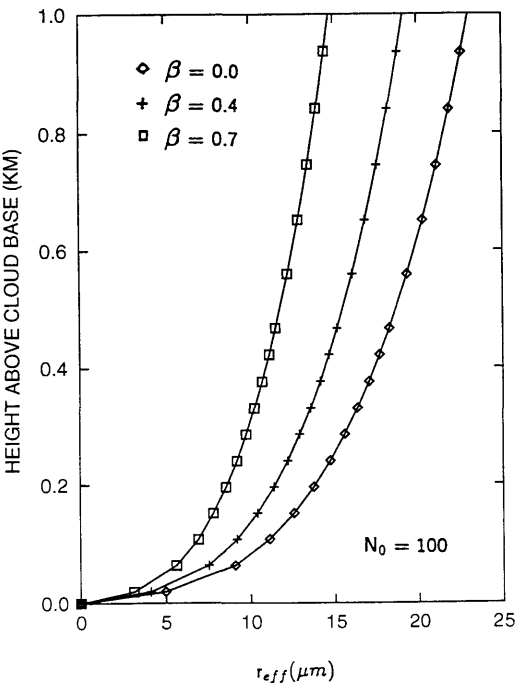

Fig. 2. Variation of the effective radius of droplets as a function of height above cloud base for different values of the mixing parameter β. The droplet concentration N was set to 100 cm^{-3}.

It is assumed in the derivations given in the *Appendix* that the droplet number concentration N is independent of height. Although there is some evidence to suggest that this is the case (Slingo et al., 1982), there are a number of factors acting to counter this. These include evaporation, drizzle, supersaturation, and the availability of CCN in the air parcels mixed into the top of the cloud. All these factors act in a complex way to influence N near the cloud top (Jensen et al., 1985), so that the assumption that N is independent of height is not strictly valid. However, this study is based on the idea that the primary response to changed solar absorption is a change in convective mixing, which can be linked to the microphysics using the parameter β. Hence, in the context of the prima facie estimates presented here, the factors mentioned above are considered to be of secondary importance.

Estimates of cloud reflectance and absorptance require a knowledge of the single scattering albedo $\bar{\omega}$ in addition to the optical depth τ. The functional dependence of $\bar{\omega}$ is illustrated by the approximation found by Ackerman and Stephens (1987), who showed that

$$1 - \bar{\omega} \simeq c\kappa r_{\text{eff}}^{p}, \tag{6}$$

where κ is the bulk absorption coefficient of water, p is a parameter which depends on the strength of the absorption in the waveband under consideration, and c is a constant. Eq. (6) therefore relates $\bar{\omega}$ to the same parameters as τ through eq. (5).

2.3. *Effect of solar absorption on cloud structure*

Given the functional dependences derived above, it is next necessary to understand the effect of changes in solar absorption on variables such as the mixing parameter β and geometrical cloud thickness h.

The effect of variations in solar absorption is apparent in the diurnal cycle of stratocumulus clouds. In particular, it has become clear through a combination of observational and modelling studies that solar absorption during the daytime acts to reduce the moisture content of the cloudy layer (Nicholls, 1984; Nicholls and Leighton, 1986; Turton and Nicholls, 1987). The variety and complexity of the mechanisms responsible for this drying have been stressed by Driedonks and Duynkerke (1989). Nevertheless, the primary mechanism is undoubtedly the decoupling of the cloud from the sub-cloud layer due to the reduction in radiative cooling at the cloud top. This cooling is responsible for the convective mixing of the entire boundary layer at night. The reduction of this mixing during the day not only reduces the upward transport of water vapour into the cloud, but leads to the establishment of a local circulation confined to the cloudy layer. This circulation is driven by the interplay of radiative cooling and warming in the cloud, with cooling dominant near the cloud top, and solar heating more uniformly distributed down into the cloud. Hence, entrainment of overlying air continues, but with a marked reduction in the supply of water vapour.

The consequences of these changes are reductions in both cloud liquid water content and geometrical thickness. For example, a simulation by Turton and Nicholls (1987) showed a cloud of initial thickness 500 m reduced to 250 m in the course of 8 hours of insolation. If, as suggested

above, $\tau \propto h^{5/3}$, then the implied reduction in τ is by 70%. Additional support for this picture was provided by the measurements of Betts (1990), who found evidence for decoupling associated with convective mixing in stratocumulus layers during the daytime. Further measurements of the diurnal variation of stratocumulus were recently reported by Albrecht et al. (1990) and Blaskovic et al. (1991). Their findings indicated that both the column liquid water content and geometrical cloud thickness decreased during the daytime, each to $\sim 50\%$ of its overnight maximum.

The evidence therefore suggests that the absorption of solar radiation acts to reduce cloud geometrical thickness and liquid water content through an internal mechanism which is based on a qualitative change in circulation within the boundary layer. Equation (3) indicates that a reduction in liquid water content connotes an increase in β. Thus, the implication for the present work is that if the solar absorption increases due to a change in droplet number density, then the effects described above will act to simultaneously increase the mixing parameter β and to reduce the geometrical cloud thickness h.

3. Radiative transfer in stratocumulus clouds

In this section, we employ the functional dependences obtained above in order to evaluate the effect of the internal feedback mechanism previously described. This is approached in two stages. First, approximations valid in the limiting cases of optically thin and thick clouds are employed to gain a qualitative appreciation of the operation of the effect. Following this, a two stream radiative transfer model is used to determine conditions under which the behaviour encountered in the limiting cases is applicable to realistic boundary layer clouds.

3.1. Limiting cases

As discussed by King and Harshvardhan (1986), a thin cloud is one for which the approximation of single scattering holds, whilst for a thick cloud the asymptotic theory provides an adequate radiative transfer approximation. From the calculations of King and Harshvardhan (1986) it can be inferred that for a thin cloud, $\tau \leqslant 0.1$, while for a thick cloud $\tau \geqslant 15$. Since most stratus clouds have an optical depth between 1 and 15, this definition leaves the stratocumulus clouds in an intermediate range between the thick and thin limit. However, in these limits, radiative transfer theory allows for elegant approximations to absorptance on which simple arguments can be constructed to identify the manner in which absorption will change as the droplet number concentration is increased. Detailed numerical calculations can then be performed to support the simple theory and to explore the intermediate range of optical depths.

3.1.1. Thin limit. Absorptance in the thin cloud limit is given by:

$$a \sim \frac{\tau(1-\bar{\omega})}{\mu_0}, \tag{7}$$

(see, for example, Preisendorfer, 1976). Substitution of equations (4), (5) and (6) yields

$$a \sim \frac{[(1-\beta)^{2+p} h^{5+p} N^{1-p}]^{1/3}}{\mu_0}. \tag{8}$$

The response of absorptance to increasing droplet number density N results from a competition between increased optical depth ($\tau \propto N^{1/3}$) and reduced single particle absorption ($1-\bar{\omega} \propto N^{-p/3}$). Since for water clouds in the shortwave $0 \leqslant p \leqslant 1$ (Ackerman and Stephens, 1987), it follows that the optical depth effect prevails, so that the absorptance increases with N. In addition, the absorptance also increases with increasing solar zenith angle (decreasing μ_0).

The response of an optically thin cloud to increasing droplet number density N is therefore as follows. Initially, the increase in N will induce an increase in absorptance a. However, as described in the previous section, increased absorptance will lead to an increase in the mixing parameter β, coupled with a decrease in geometrical cloud thickness h. In view of eq. (8), this implies decreased absorptance, and hence the feedback is negative.

The conclusion is that enhancement of solar absorption due to increasing the droplet concentration is at least in part compensated for by changes to the internal dynamic and thermodynamic structure. In other words, the cloud contains a self-regulating mechanism which counteracts a move away from absorption equilibrium. This absorption feedback has the consequent effect

of decreasing the optical depth and therefore the cloud reflectance, so that in the thin limit the increase in cloud albedo due to increased droplet concentration is partly offset.

3.1.2. Thick limit. Twomey and Bohren (1980) have shown that in the optically thick limit,

$$a \sim (1-\bar{\omega})^{1/2} H(\mu_0), \tag{9}$$

where H is the function introduced by Chandrasekhar (1950) in problems involving semi-infinite atmospheres. Although H is notated as a function of μ_0 only, it is also dependent on $\bar{\omega}$. However, Twomey and Bohren (1980) have shown that H varies only weakly with $\bar{\omega}$ when $(1-\bar{\omega})$ is small, as is the case for cloud water droplets. Thus,

$$a \sim (1-\beta)^{p/6} h^{p/6} N^{-p/6} H(\mu_0), \tag{10}$$

Hence, in the thick limit, an increase in droplet concentration causes an initial *decrease* in absorptance. This leads to a decrease in the mixing parameter β, and a thickening of the cloud layer (increased h), both of which act to *increase* the absorptance from its initial downward perturbation. Hence, although the initial direction of the perturbation is opposite to the optically thin limit, the feedback is once again negative in the sense that the absorptance is stabilized. However, the changes in β and h now have the effect of increasing the optical depth τ from its value in the absence of feedback. Hence the absorption feedback acts to enhance the cloud reflectance in the thick limit.

3.2. Detailed calculations

The cases examined above indicate the operation of absorption feedback under conditions of limiting optical depth. However, it is not obvious whether these cases are at all representative of realistic boundary layer clouds. Hence, in this section we use detailed radiative transfer calculations to model the behaviour of stratocumulus clouds, with the aim of defining conditions under which the limiting behaviour found above, and thus the associated feedback effect, is likely to be applicable.

The radiative transfer calculations are based on the delta-Eddington two stream approximation of Joseph et al. (1976). An important aspect of the model development was the inclusion of realistic cloud microphysics to simulate the variations in absorption characteristics as a result of perturbations in N. We adopted the approach of Slingo and Schrecker (1982), who divided the solar spectrum into 24 intervals. Horizontal path transmittances were calculated for ozone and water vapour, and the transmittances were weighted by the solar spectrum and fitted by the sum of decaying exponentials using a non-linear regression software package.

Our approach differs from that of Slingo and Schrecker in two respects. Firstly, by imposing a lesser constraint of accuracy of the fits (three significant digits rather than four) we were able to reduce the total number of times the delta-Eddington routine needs to be called from 141 times to 75. This lesser accuracy is justified as the inaccuracies inherent in the delta-Eddington approach (up to 20%, King and Harshvardhan (1986)) overwhelm any small perturbation in transmittance. Secondly, the parameterization of the microphysical parameters $\bar{\omega}$, τ, and the scattering asymmetry factor g was modified so as to accomodate our model of cloud microphysics as expressed by eqs. (2)–(6).

The single scattering albedo $\bar{\omega}$ was parameterized by eq. (6), the extinction coefficient σ was $\sigma/N = a_1 r_{\text{eff}}^{b_1}$ and g as $g = a_2 r_{\text{eff}}^{b_2}$, with a_1, a_2, b_1, and b_2 constants. For each layer in the cloud, the optical depth was calculated as $\tau = \sigma \Delta z$ with Δz the thickness of the layer. For different values of β, h and N Mie-calculations were performed for 10 wavelengths in each of the 24 spectral bands. The values for ω_0, σ, and g were weighted using the procedure outlined by Slingo and Schrecker, and fitted to our parameterization. The fits were determined over the range $4.0\ \mu\text{m} \leqslant r_{\text{eff}} \leqslant 25\ \mu\text{m}$.

Next, clouds of thickness ranging from 50 to 1000 m were embedded in a midlatitude summertime atmosphere with 20% relative humidity up to 10 km, and climatology above. The boundary layer was considered to be well mixed with a liquid water potential temperature $\theta_\ell = 287$ K, and a total water mixing ratio of 0.008 kg kg^{-1}. These values give a cloud base height of a little over 500 m. The top of the cloud was considered the top of the boundary layer with a change of the boundary layer temperature and humidity to those of the dry upper atmosphere from one level to the next. Such conditions can be considered as typical for stratus clouds. Spectrally integrated reflectances r and absorptances a were calculated for 20 values of the parameter μ_0.

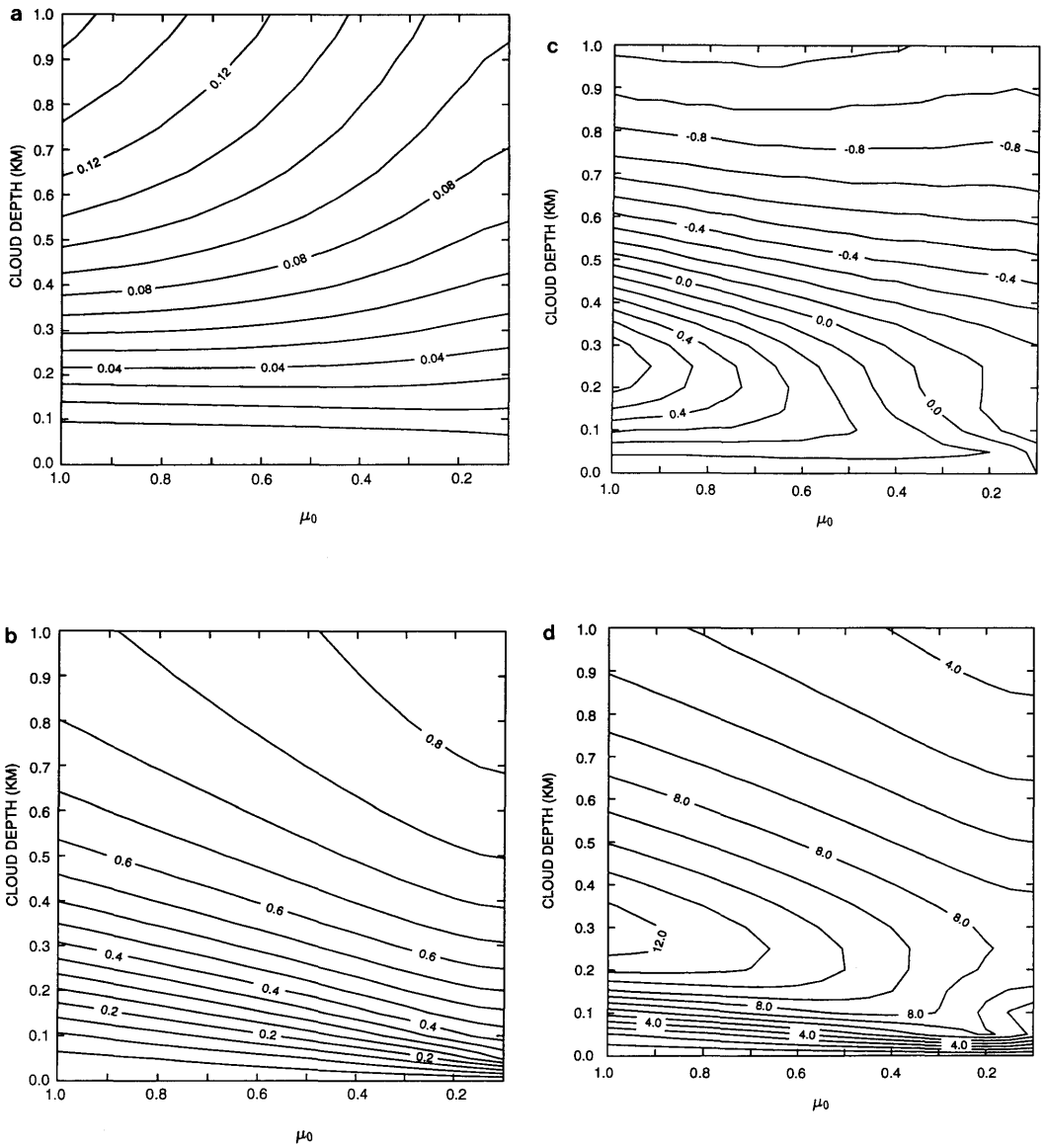

Fig. 3. (a) Isoline plot of cloud absorptance a as a function of solar zenith cosine μ_0 and geometrical cloud thickness h. The plot shows a demarcation between optically thin and thick behaviour at $h \sim 200$ m. The assumed values of droplet concentration and mixing parameter were $N = 50\ \text{cm}^{-3}$ and $\beta = 0$. (b) Isoline plot of cloud reflectance r as a function of solar zenith cosine μ_0 and geometrical cloud thickness h. The plot shows a general trend toward higher reflectance for thicker clouds and for sun angles away from zenith. The assumed values of droplet concentration and mixing parameter were $N = 50\ \text{cm}^{-3}$ and $\beta = 0$. (c) Isoline plot of the % difference in absorptance due to an increase in droplet concentration from $50\ \text{cm}^{-3}$ to $150\ \text{cm}^{-3}$. Optically thin behaviour is apparent in the increase in absorptance seen in the lower left portion of the plot. The assumed value of the mixing parameter was $\beta = 0$. (d) Isoline plot of the % difference in reflectance due to an increase in droplet concentration from $50\ \text{cm}^{-3}$ to $150\ \text{cm}^{-3}$. The greatest increase in reflectance coincides with the largest increase in absorptance seen in Fig. 3c. The assumed value of the mixing parameter was $\beta = 0$.

A distinguishing feature of the optically thin and thick limits is the dependence of absorptance a on sun zenith cosine μ_0. In the optically thin limit, $a \propto \mu_0^{-1}$, while in the thick limit, $a \propto H(\mu_0)$. Twomey and Bohren (1980) have shown that H increases with increasing μ_0, implying a dependence of absorptance on μ_0 opposite to that for the optically thin case. Hence our results are presented as isoline plots in the (μ_0, h) plane. In these plots, the μ_0 dependence can be used to discriminate optically thin and thick behaviour, while the dependence on h delineates regimes of geometrical cloud thickness over which the limiting behaviour is found to apply.

Fig. 3a shows such an isoline plot of a_{50}, the absorptance calculated for a droplet concentration of $N = 50\ \text{cm}^{-3}$. The value of $50\ \text{cm}^{-3}$ was chosen to represent "clean" oceanic conditions. A mixing parameter of $\beta = 0$ was assumed. The figure indicates that the absorptance behavior as found for the thin limit extends into the stratocumulus regime for clouds of geometrical thickness less than 250 m. In this regime, the absorptance is found to increase with decreasing μ_0, albeit weakly. For cloud depths over 250 m the thick regime becomes apparent, since absorptance decreases with decreasing μ_0. Fig. 3b shows the cloud top reflectance r_{50}. This plot indicates a general increase in reflectance toward small solar zenith cosines and for thicker clouds. Also, the reflectance of very thick clouds is relatively insensitive to variations in either μ_0 or h. For both Figs. 3a, b, increasing β results in similar plots, but with reduced values of reflectance and absorptance as liquid water content is diminished following eq. (2).

An additional distinction between the optically thin and thick limits is the sense of the perturbation in absorptance caused by a change in droplet concentration N. In the thin limit, an increase in N is expected to cause an increase in absorptance (eq. (8)), and vice versa in the thick limit (eq. (10)). Perturbations in absorptance and reflectance were calculated by increasing N from $50\ \text{cm}^{-3}$ to $150\ \text{cm}^{-3}$. This relatively large increment was adopted in order to amplify the magnitude of the perturbations in absorptance and reflectance for display purposes. Fig. 3c shows the absorptance difference $a_{150} - a_{50}$ (%). There exist a region where indeed cloud absorptance is increased, as would be expected in the optically thin limit. This region is most pronounced toward the lower left of the diagram, corresponding to thin clouds and sun angles near the zenith.

Fig. 3d shows the reflectance difference $r_{150} - r_{50}$. There is a maximum perturbation of a little over 12% for cloud thicknesses of 300 m and overhead sun. The maximum coincides with the region of greatest increase in absorptance as seen in Fig. 3c.

In summary, detailed calculations do indeed delineate regimes where the absorptance of stratocumulus clouds follows the behaviour predicted in the optically thin and thick limits. For the cases studied, optically thin behaviour is found for clouds with geometrical thicknesses below a threshold value in the range 250–300 m, corresponding to an optical depth threshold of $\tau \sim 10$.

4. Impact of absorption feedback on climate

Since we are now in the position to indicate the manner in which cloud reflectance is altered as a result of the absorption feedback, it also possible to estimate the impact of the absorption feedback on the global mean radiative forcing perturbation due to changes in the droplet concentration. Charlson et al. (1987, 1992) related the net cloud top perturbation in reflectance Δr_{ct} linearly to the mean top of the atmosphere reflectance, the global mean albedo perturbation and also the global mean radiative forcing. The question is: how is this forcing altered through the absorption feedback?

While an exact calculation of the albedo perturbation due to the absorption feedback is beyond the scope of the present paper, it is nevertheless possible to make an order-of-magnitude estimate. To do this, we note that the absorption feedback always acts to restore the cloud absorptance toward its unperturbed value. Somewhat intuitively, we suppose that the feedback is exactly sufficient to cancel the perturbation in absorptance caused by the increase in droplet concentration. We then calculate the effect of this degree of absorption feedback on the cloud top reflectance.

Specifically, we write the absorptance as a function of the three variables material to the absorption feedback,

$$a \equiv a(N, h, \beta). \tag{11}$$

The exact cancellation proposed above implies that

$$\delta a = \frac{\partial a}{\partial N}\delta N + \frac{\partial a}{\partial h}\delta h + \frac{\partial a}{\partial \beta}\delta\beta = 0, \tag{12}$$

where the partial derivatives with respect to a given variable imply that the remaining two are held constant. This equation can be viewed as expressing the combined perturbation in h and β required to nullify the response of the absorptance to a given change in N. Since it is not clear how the changes in h and β will be apportioned, each effect is considered separately. That is, increments δh and $\delta\beta$ were independently calculated from

$$\delta h = -\frac{\partial a}{\partial N}\delta N\left(\frac{\partial a}{\partial h}\right)^{-1}, \tag{13}$$

$$\delta\beta = -\frac{\partial a}{\partial N}\delta N\left(\frac{\partial a}{\partial \beta}\right)^{-1}. \tag{14}$$

In each case, the calculated increment δh or $\delta\beta$ represents the change required to counterbalance unilaterally the increase in absorptance due to the change in N. The partial derivatives required in this calculation were obtained from the model described in Subsection 3.2 using finite differences.

The effect of the absorption feedback on the cloud top reflectance is obtained by expressing the total reflectance perturbation as

$$\delta r = \frac{\partial r}{\partial N}\delta N + \frac{\partial r}{\partial h}\delta h + \frac{\partial r}{\partial \beta}\delta\beta. \tag{15}$$

In the absence of feedback, the change in reflectance is simply

$$\delta r_0 = \frac{\partial r}{\partial N}\delta N \tag{16}$$

which represents the standard Twomey effect. By separate calculation of the increments δh and $\delta\beta$ from eqs. (13) and (14), alternative estimates may be obtained of the reflectance perturbation with feedback included:

$$\delta r_1 = \frac{\partial r}{\partial N}\delta N + \frac{\partial r}{\partial h}\delta h, \tag{17}$$

$$\delta r_2 = \frac{\partial r}{\partial N}\delta N + \frac{\partial r}{\partial \beta}\delta\beta. \tag{18}$$

The results from these calculations are shown in Fig. 4. The perturbation δN was taken to be a 30% increase from 50 to 65 cm^{-3}. A sun zenith angle of 60° was adopted as a representative global average. The solid line in Fig. 4 represents the variation of δr_0 with geometrical cloud thickness, while the dashed line represents δr_1. It was found that $\delta r_2 \simeq \delta r_1$, so only the latter is presented.

As anticipated, the absorption feedback acts to diminish the standard Twomey effect perturbation δr_0 for thin clouds, while enhancing it for thick clouds. The transition thickness is ~350 m. For thin clouds of $h \sim 100$ m, the reflectance perturbation is reduced from $\delta r_0 \simeq 1.8\%$ to $\delta r_1 \simeq 1.2\%$, or by -30% of the standard value. For thick clouds of $h \sim 1000$ m, the reflectance perturbation is *increased* from $\delta r_0 \simeq 1.1\%$ to $\delta r_1 \simeq 1.7\%$, a change of over $+50\%$. As stated above, these perturbations are linearly related to the global mean radiative forcing, which Charlson et al. (1992) found to be -2 W m^{-2} for a 30% global increase in droplet concentration. Hence the inclusion of feedback implies a revised estimate of forcing of

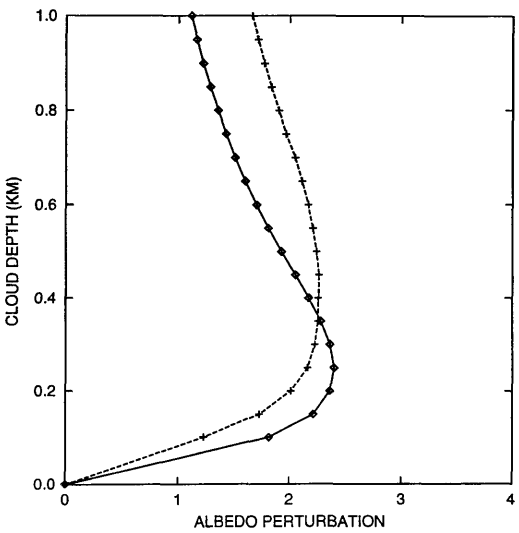

Fig. 4. Comparison of perturbation in reflectance with and without absorption feedback. The solid line indicates the reflectance perturbation δr_0 arising from a 30% increase in droplet concentration, from 50 to 65 cm^{-3}, in the absence of feedback. The dashed line shows the perturbation δr_1 arising from the same increment in droplet concentration, but with absorption feedback included.

between $-1.3\ \mathrm{W\,m^{-2}}$ and $-3.0\ \mathrm{W\,m^{-2}}$ depending on cloud thickness. This represents a substantial modification to the standard picture, and shows that feedback mechanisms internal to the cloud have a significant potential impact on the magnitude of climate forcings.

5. Conclusion

This paper has shown that increasing the droplet concentration in marine boundary layer clouds triggers an internal feedback mechanism which modifies the increase in reflectance predicted in previous studies. The feedback mechanism stems from the effect of changed solar absorption on mixing between the cloud and overlaying dry air, and hence on the microphysics of the cloud droplets. It was shown that the feedback operates quite differently in optically thin and thick clouds. For stratocumulus layers with optical depth $\leqslant 10$ (geometrical thickness $\leqslant 300$ m) the feedback partly offsets the reflectance increase due to the increase in droplet concentration. By contrast, for optically thick clouds the reflectance is further enhanced.

Based on simplifying assumptions, the estimated modification to the reflectance perturbation following from a 30% increase in droplet concentration is in the range -30% for thin clouds, to $+50\%$ for thick clouds. These changes apply linearly to the climate forcing caused by boundary layer clouds, and highlight the potential significance of the effect. In practice, definite conclusions are difficult to draw in view of the large variability of stratocumulus cloud thickness and coverage. However, a large portion of the oceans is known to be covered by optically thin stratocumulus. The present work suggests that, in the event of increasing droplet concentration, the reflectance enhancement for this component will be somewhat less than expected from the previous work of Twomey and others.

In this study, attention has been focused on the effect of changing droplet concentration on the absorption of solar radiation within clouds. However, it is well known that changed droplet concentration affects other properties of the cloud, notably the significance of drizzle, and hence the ability of the cloud the retain its liquid water (Albrecht, 1989). Also, modelling studies have shown that drizzle may significantly affect the entrainment rate at the top of the cloud and therefore will influence cloud decoupling and cloud thickness (Turton and Nicholls, 1987). Clearly, attention should be given to the phenomenon of drizzle in future modelling efforts.

Observationally, it is important to attempt to establish a relation between CCN concentration and cloud reflectance under homogeneous conditions. This is one of the primary aims of the Southern Ocean Cloud Experiment (SOCEX), an initiative of CSIRO Division of Atmospheric Research, which is about to commence with instrumented flights over the Southern Ocean to the southwest of Tasmania.

6. Appendix

Mixing parameter and microphysics

This appendix gives the derivation of the functional forms of optical depth τ and effective droplet radius r_{eff}, as quoted in Subsection 2.2. This is achieved by first calculating the height dependence of the droplet concentration N.

The mixing parameter β was introduced by Betts (1985) to quantify the extent of mixing between the moist boundary layer and the overlaying dry atmosphere. Defining $M(z)$ as a proxy for one of the conserved variables θ_{e} (equivalent potential temperature), θ_{ℓ} (liquid water potential temperature) or q_{T} (total water mixing ratio), the height variation of any of these may be written

$$\frac{\mathrm{d}M}{\mathrm{d}z} = \beta \left(\frac{\partial M}{\partial z_*} \right)_{\mathrm{LT}}, \tag{19}$$

where z_* is the saturation height and the subscript LT denotes the mixing line on a conserved variable diagram, connecting the thermodynamic state of the unmixed boundary layer (L) with that of unmixed overlying air (T). Mixing as described here refers to entrainment of dry warm parcels into the cloudy boundary layer from the top. β used in (19) is the height equivalent of (1).

Assuming linear variations over the vertical extent of the cloud, integration of equation (19) from the bottom of the cloud to some height z within the cloud yields

$$M(z) = M_{\mathrm{L}} + \beta \frac{(M_{\mathrm{T}} - M_{\mathrm{L}})}{(z_{*\mathrm{T}} - z_{*\mathrm{L}})} (z - z_{\mathrm{B}}). \tag{20}$$

where z_{*L} and z_{*T} refer respectively to the saturation heights of the unmixed cloud layer, and unmixed overlying air. The saturation height of the unmixed cloud layer is exactly equal to the cloud base level; $z_{*L} = z_B$.

Equation (20) may be written in the alternative form

$$M(z) = f(z)\, M_L + [1 - f(z)]\, M_T, \tag{21}$$

where $f(z)$ represents the fraction of unmixed boundary layer air, and $1 - f(z)$ is the fraction of unmixed overlying air present at height z. Comparison of eqs. (20) and (21) shows that

$$f(z) = 1 - \beta \frac{(z - z_B)}{z_{sc}} \tag{22}$$

where z_{sc} is a scaling height defined as

$$z_{sc} = z_{*T} - z_B. \tag{23}$$

In order to derive the height dependence of the droplet concentration, two assumptions are made. The first is that the conversion of CCN into droplets occurs exclusively at cloud base. The second is that the droplet concentration is not depleted as a result of evaporation due to mixing. These assumptions imply that, in the absence of mixing, the droplet concentration is independent of height, thus behaving as a conserved variable. Hence, in the presence of mixing, the height dependence will follow equation (21). Since there are no droplets in the overlying air, the height dependence of droplet concentration is simply

$$N(z) = N_0 f(z), \tag{24}$$

where $N_0 \equiv N(z_B)$ is the droplet concentration at cloud base.

The functional dependences of cloud optical depth and effective droplet radius are now derived. These hinge on relating the liquid water content to the droplet size distribution and its moments. Regarding the droplet size distribution, it is convenient to adopt the well known gamma distribution, which has been used extensively in the past to represent droplet size distributions in clouds (e.g., Diermendjian, 1969). Thus,

$$n(r, z) = a(z)\, r(z)^{\alpha} \exp[-b(z)\, r(z)], \tag{25}$$

where n is the droplet concentration density, r is the droplet radius, and $a(z)$, $b(z)$, and α are the parameters of the distribution function. Note that, in principle, α is also a function of height. However, there is insufficient information available to constrain α, which is therefore assumed to be independent of height. The sensitivity of the results to this assumption is considered below.

The droplet concentration N is given by

$$N(z) = \int_0^{\infty} \mathrm{d}r n(r, z) = a(z)\, b(z)^{-(\alpha+1)}\, \Gamma(\alpha + 1), \tag{26}$$

where Γ is the gamma function. The volume of liquid water per unit volume of air is

$$\mathscr{V}(z) = \frac{4}{3}\pi \int_0^{\infty} \mathrm{d}r r^3 n(r, z) = \frac{4}{3}\pi a(z)\, b(z)^{-(\alpha+4)}\, \Gamma(\alpha + 4), \tag{27}$$

which is related to the liquid water mixing ratio defined in equation (3) by

$$w(z) = \rho_w \mathscr{V}(z) \tag{28}$$

where ρ_w is the bulk density of water. Substitution from (28) into (27) using (3) defines the parameter $b(z)$ as

$$b^{-1}(z) = [(1 - \beta)\, A_d (z - z_B)]^{1/3} \times [\tfrac{4}{3}\pi \rho_w N(z)]^{-1/3} \times [(\alpha + 3)(\alpha + 2)(\alpha + 1)]^{-1/3}, \tag{29}$$

where the gamma function has been replaced by the identity $\Gamma(n + 1) = n!$. Substitution in (26) for $b(z)$ allows the evaluation of $a(z)$. With the evaluation of $a(z)$ and $b(z)$, the calculation of optical depth and effective radius is straightforward.

The optical depth τ can be found by integrating the volume extinction coefficient σ over height:

$$\tau = \int_{z_B}^{z_T} \mathrm{d}z \sigma(z), \tag{30}$$

where

$$\sigma(z) = \pi Q \int_0^\infty \mathrm{d}r r^2 n(r, z)$$

$$= \pi Q b(z)^{-2} N(z)(\alpha+2)(\alpha+1), \tag{31}$$

where Q is the droplet extinction efficiency. For droplets large compared with the wavelength, $Q \simeq 2$. Substitution in (31) for $b(z)$ and $N(z)$ gives

$$\sigma(z) = \pi^{1/3} Q \left(\frac{4}{3}\rho_w\right)^{-2/3} \mathscr{A}(\alpha)[(1-\beta) A_d]^{2/3}$$

$$\times N_0^{1/3}(z - z_B)^{2/3}\left[1 - \beta\frac{(z-z_B)}{z_{sc}}\right]^{1/3}, \tag{32}$$

where

$$\mathscr{A}(\alpha) = \left[\frac{(\alpha+2)(\alpha+1)}{(\alpha+3)^2}\right]^{1/3}. \tag{33}$$

The integral of σ over height does not admit an analytic solution. However, as discussed below, the scale height z_{sc} is generally large compared with $(z - z_B)$, so that

$$\beta\frac{(z-z_B)}{z_{sc}} < 1. \tag{34}$$

Expanding the term in large square brackets in eq. (32) as a first order Taylor series, and integrating over height to obtain the optical depth then yields

$$\tau = \frac{3}{5}\pi^{1/3} Q \left(\frac{4}{3}\rho_w\right)^{-2/3} \mathscr{A}(\alpha)[(1-\beta) A_d]^{2/3}$$

$$\times N_0^{1/3} h^{5/3}\left(1 - \frac{5}{24}\beta\frac{h}{z_{sc}}\right), \tag{35}$$

where h is the geometrical cloud thickness.

The effect of the bracketed term at the right hand end of the above equation is small, since typical boundary layer scale heights are in the range $1000\ \mathrm{m} \leqslant z_{sc} \leqslant 3000\ \mathrm{m}$, while the geometrical cloud thickness $h < 1000$ m. Taking a worst-case situation where $h = z_{sc}$ and a typical value of $\beta = 0.4$, the departure of the bracketed term from unity is $\sim 8\%$. This discrepancy is not significant in the present context.

The sensitivity to variations in α was examined by comparing optical depths obtained for $\alpha = 7$, as used in most of our calculations, with those obtained for $\alpha = 2$. The change in optical depth was 15%. Although significant, such large variation in α over the vertical extent of a given cloud is most unlikely.

The vertical gradient of liquid water mixing ratio, A_d, was assumed constant in the present study. Although valid locally, A_d is known to vary considerably with latitude. This should be borne in mind for future studies comparing cloud properties in widely different latitude zones.

Collecting constants in (35), and approximating the final bracketed term by 1, leads to the expression

$$\tau = C_1(1-\beta)^{2/3} N^{1/3} h^{5/3}, \tag{36}$$

where N_0 has been replaced by N for notational convenience.

The effective radius r_{eff} is defined as

$$r_{eff}(z) = \frac{\int_0^\infty \mathrm{d}r r^3 n(r, z)}{\int_0^\infty \mathrm{d}r r^2 n(r, z)}$$

$$= b(z)^{-1}(\alpha+3). \tag{37}$$

Substitution from eq. (29) and collection of constants yields

$$r_{eff}(z) = C_2(1-\beta)^{1/3}(z - z_B)^{1/3}$$

$$\times N_0^{-1/3}\left[1 - \beta\frac{(z-z_B)}{z_{sc}}\right]^{-1/3}. \tag{38}$$

Once again, the term in large square brackets may be expanded as a first order Taylor series, giving $[1 + \frac{1}{3}\beta(z - z_B)/z_{sc}]$. In this case the approximation involved in neglecting the linear term leads to a maximum relative error of $\sim 13\%$ for $z - z_B = z_{sc}$ and $\beta = 0.4$. Hence the dominant functional dependence is retained by approximating the term in square brackets by 1, and the effective radius becomes

$$r_{eff}(z) = C_2(1-\beta)^{1/3}(z - z_B)^{1/3} N^{-1/3}, \tag{39}$$

where again N_0 has been replaced by N for notational convenience.

REFERENCES

Ackerman, S. A. and Stephens, G. 1987. The absorption of solar radiation by cloud droplets: An application of anomalous diffraction theory. *J. Atmos. Sci.* **44**, 1574–1588.

Albrecht, B. A. 1989. Aerosol, Cloud microphysics, and fractional cloudiness. *Science* **245**, 1227–1230.

Albrecht, B. A., Fairall, C. W., Thomson, D. W., White, A. B. and Snider, J. B. 1990. Surface-based remote sensing of the observed and adiabatic liquid water content of stratocumulus clouds. *Geophys. Res. Let.* **17**, 89–92.

Betts, A. K. 1985. Mixing line analysis of clouds and cloudy boundary layers. *J. Atmos. Sci.* **42**, 2751–2763.

Betts, A. K. 1990. Diurnal variation of California coastal stratocumulus from two days of boundary layer soundings. *Tellus* **42A**, 302–304.

Betts, A. K. and Boers, R. 1990. A cloudiness transition in a marine boundary layer. *J. Atmos. Sci.* **47**, 1480–1497.

Blaskovic, M., Davies, R. and Snider, J. B. 1991. Diurnal variation of marine stratocumulus over San Nicholas Island during July 1987. *Mon. Wea. Rev.* **119**, 1469–1478.

Boers, R. and Betts, A. K. 1988. Saturation point structure of marine stratocumulus clouds. *J. Atmos. Sci.* **45**, 1156–1175.

Boers, R., Melfi, S. H. and Palm, S. P. 1991. Cold-air outbreak during GALE: Lidar observations and modeling of boundary layer dynamics. *Mon. Wea. Rev.* **119**, 1132–1150.

Chandrasekhar, S. 1950. *Radiative transfer.* Oxford University Press, Oxford.

Charlson, R. J., Lovelock, J. E., Andreae, M. O. and Warren, S. G. 1987. Oceanic phytoplankton, atmospheric sulphur, cloud albedo and climate. *Nature* **326**, 655–661.

Charlson, R. J., Schwartz, S. E., Hales, J. M., Cess, R. D., Coakley, J. A., Hansen, J. E. and Hoffmann, D. J. 1992. Climate forcing by anthropogenic aerosols. *Science* **255**, 423–430.

Diermendjian, D. 1969. *Electromagnetic scattering on spherical polydispersions.* Elsevier, New York.

Driedonks, A. G. M. and Duynkerke, P. G. 1989. Current problems in the stratocumulus-topped atmospheric boundary layer. *Boundary Layer Meteor.* **46**, 275–303.

Hudson, J. G. 1991. Observations of anthropogenic cloud condensation nuclei. *Atmos. Environment* **25A**, 2449–2455.

Jensen, J. B., Austin, P. H., Baker, M. B. and Blyth, A. M. 1985. Turbulent mixing, spectral evolution and dynamics in a warm cumulus cloud. *J. Atmos. Sci.* **42**, 173–192.

Joseph, J. H., Wiscombe, W. J. and Weinman, J. A. 1976. The delta-Eddington approximation for radiative flux transfer. *J. Atmos. Sci.* **33**, 2452–2459.

King, M. D. and Harshvardhan, 1986. Comparative accuracy of selected multiple scattering approximations. *J. Atmos. Sci.* **43**, 784–801.

Nicholls, S. 1984. The dynamics of stratocumulus: aircraft observations and comparison with a mixed layer model. *Quart. J. Roy. Meteor. Soc.* **110**, 783–820.

Nicholls, S. and Leighton, J. 1986. An observational study of the structure of stratiform cloud sheets. Part I. Structure. *Quart. J. Roy. Meteor. Soc.* **112**, 431–460.

Preisendorfer, R. W. 1976. *Hydrological optics*, vol. 1. NOAA, Joint Tsunami Research Effort, Honolulu, HI, 218 pp.

Radke, L. F., Coakley, J. A. and King, M. D. 1989. Direct and remote sensing observations of the effects of ships on clouds. *Science* **246**, 1146–1149.

Randall, D. A. 1984. Outlook for research on subtropical marine stratiform clouds. *Bull. Amer. Meteor. Soc.* **65**, 1290–1301.

Slingo, A., Nicholls, S. and Schmetz, J. 1982. Aircraft observations of marine stratocumulus during JASIN. *Quart. J. Roy. Meteor. Soc.* **108**, 833–856.

Slingo, A. and Schrecker, H. M. 1982. On the shortwave radiative properties of stratiform water clouds. *Quart. J. Roy. Meteor. Soc.* **108**, 407–426.

Turton, J. D. and Nicholls, S. 1987. A study of the diurnal variation of stratocumulus using a multiple mixed-layer model. *Quart. J. Roy. Meteor. Soc.* **113**, 969–1009.

Twomey, S. A. 1977. The influence of pollution on the shortwave albedo of clouds. *J. Atmos. Sci.* **34**, 1149–1152. (check)

Twomey, S. A. and Bohren, C. F. 1980. Simple approximations for calculations of absorption in clouds. *J. Atmos. Sci.* **37**, 2086–2094.

Twomey, S. A., Piepgrass, M. and Wolfe, T. L. 1984. An assessment of the impact of pollution on global cloud albedo. *Tellus* **36B**, 356–366.